TRANSADAPTER: VISION TRANSFORMER FOR FEATURE-CENTRIC UNSUPERVISED DOMAIN ADAPTATION

Anonymous authors
Paper under double-blind review

ABSTRACT

Unsupervised Domain Adaptation (UDA) aims to leverage labeled data from a source domain to address tasks in a related but unlabeled target domain. This problem is particularly challenging when there is a significant gap between the source and target domains. Traditional methods have largely focused on minimizing this domain gap by learning domain-invariant feature representations using convolutional neural networks (CNNs). However, recent advances in vision transformers, such as the Swin Transformer, have demonstrated superior performance in various vision tasks. In this work, we propose a novel UDA approach based on the Swin Transformer, introducing three key modules to improve domain adaptation. First, we develop a Graph Domain Discriminator that plays a crucial role in domain alignment by capturing pixel-wise correlations through a graph convolutional layer, operating on both shallow and deep features in the transformer. This module also calculates the entropy for the key attention features of the attention block to better distinguish between the source and target domains. Second, we present an Adaptive Double Attention module that simultaneously processes Windows and Shifted Windows attention to increase long-range dependency features. An attention reweighting mechanism is employed to dynamically adjust the contributions of the attention values, thereby improving feature alignment between domains. Finally, we introduce Cross-Feature Transform, where random Swin Transformer blocks are selectively transformed using our proposed transform module, enhancing the model's ability to generalize across domains by transferring the source to the target features. Extensive experiments demonstrate that our method improves the state-of-the-art on several challenging UDA benchmarks, confirming the effectiveness of our approach. In particular, our model does not include a task-specific domain alignment module, making it more versatile for various applications.

1 INTRODUCTION

Deep neural networks (DNNs) have achieved remarkable success in various machine learning tasks, particularly in computer vision (Wang et al., 2022a; Qian et al., 2021; Jiang et al., 2022; Tan et al., 2019; Chen et al., 2021b; Jiang et al., 2021). However, their performance often relies on large amounts of labeled training data, which can be costly and time-consuming to collect (Csurka, 2017; Zhao et al., 2020; Zhang et al., 2020; Oza et al., 2021). To address this, Unsupervised Domain Adaptation (UDA) has emerged as a viable alternative, transferring knowledge from a labeled source domain to an unlabeled target domain and mitigating challenges posed by domain shifts (Bousmalis et al., 2017; Kuroki et al., 2019; Wilson & Cook, 2020; VS et al., 2021).

Traditional UDA methods have used Convolutional Neural Networks (CNNs) to align source and target domains by learning transferable features across varying distributions (Kang et al., 2019; Zhang et al., 2019; Jiang et al., 2020; Li et al., 2021b). While these methods have made strides in reducing domain discrepancies through adversarial training and feature normalization, they can struggle with complex domain shifts and variability in visual patterns, highlighting ongoing challenges in domain generalization and cross-domain alignment (Morerio et al., 2020; Jiang et al., 2020).

The advent of transformers has revolutionized feature learning in both natural language processing (NLP) (Vaswani et al., 2017; Devlin et al., 2018) and computer vision (Dosovitskiy et al., 2020; Han et al., 2020; He et al., 2021; Khan et al., 2021). The Swin Transformer (Liu et al., 2021) excels in modeling long-range dependencies and processes images in non-overlapping patches, enabling effective localized adaptation. This multiscale approach is well-suited for UDA tasks, ensuring robust feature representation and precise domain alignment.

This work introduces TransAdapter, a novel framework leveraging the Swin Transformer for UDA. It addresses the limitations of traditional CNN-based methods by incorporating three key modules: a Graph Domain Discriminator, an Adaptive Double Attention module, and a Cross-Feature Transform module. These components enhance domain adaptation performance by facilitating better alignment and improving local and global feature consistency across domains.

Contributions of this paper are summarized as follows:

- The Graph Domain Discriminator captures both shallow and deep features using graph convolutional layers, enhancing pixel-wise correlation and domain alignment. we incorporate entropy in the key attention features, preventing the attention mechanism from focusing too narrowly on specific regions, leading to more balanced and transferable representations.
- The Adaptive Double Attention module captures long-range dependencies by simultaneously processing window and shifted window attention. This dual mechanism maintains global and local features, while an attention reweighting module enhances feature alignment and overall model performance.
- The Cross Feature Transform module adapts the Swin Transformer for UDA tasks. By randomly selecting a transformer block and applying a specialized transform module in each iteration, the model dynamically explores different aspects of the feature space. This enhances domain adaptation and improves performance across diverse datasets.

In summary, integrating these three modules within the Swin Transformer framework provides a robust solution for UDA, effectively addressing domain shift challenges and advancing the state-of-the-art in domain adaptation for computer vision tasks.

2 Related Work

2.1 Unsupervised Domain Adaptation (UDA) and Transfer Learning

Unsupervised Domain Adaptation (UDA) within transfer learning aims to learn transferable knowledge that is generalizable across different domains with varying data distributions. The main challenge lies in addressing the domain shift the discrepancy in the probability distributions between source and target domains.

Early UDA methods, such as Deep Domain Confusion (DDC), focused on learning domain-invariant characteristics by minimizing the maximum mean discrepancy (MMD) between two domains (Tzeng et al., 2014a). This helped align the marginal distributions of the source and target domain data at a feature level. Long et al. (Long et al., 2015b) enhanced this approach by embedding hidden representations in a reproducing kernel Hilbert space (RKHS) and applying a multiple-kernel variant of MMD to measure the domain distance more effectively. These hidden representations refer to the activations within layers of a deep neural network, where each layer captures different hierarchical features of the input data.

To further improve alignment, Long et al. (Long et al., 2017) proposed aligning the joint distributions of multiple domain-specific layers across domains using a joint maximum mean discrepancy (JMMD) metric. These layers refer to the different layers in a neural network, where each layer encodes various aspects of the data, from low-level features in earlier layers to high-level semantic information in deeper layers. The idea is to align not only the marginal distributions of individual layers but also the joint distribution of features across multiple layers, ensuring that both lower-level and higher-level representations are aligned between domains. Adversarial learning methods,

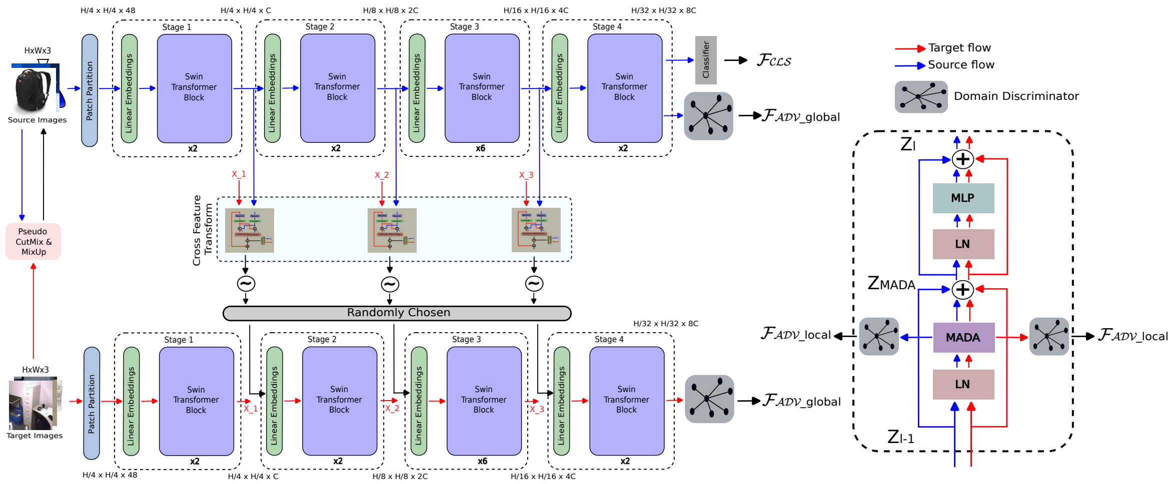

(a) Architecture (b) Swin Transformer Block

Figure 1: (a) The architecture of the proposed TransAdapter; (b) a Swin Transformer Blocks (notation presented with Eq. 4. MADA is multi-head adaptive double attention module, respectively.

inspired by GANs, have also been widely used in UDA. In these methods, an encoder is trained to generate domain-invariant features by deceiving a domain discriminator, making it unable to distinguish between the source and target domains (Goodfellow et al., 2014; Tzeng et al., 2017). This adversarial process encourages the model to learn features that generalize well across different domains, despite the domain shift.

2.2 UDA with Vision Transformers

While transformers have gained popularity in NLP, their application in UDA for vision tasks is still in its early stages. Some recent work has integrated transformers into CNNs to improve domain adaptation, focusing on critical regions of images (Xu et al., 2021a; Yang et al., 2021b). For example, methods such as cross-attention have been used to blend source and target image representations (Chen et al., 2021a), while others employ multibranch architectures to leverage self-attention and cross-attention mechanisms for feature learning and domain alignment (Saito et al., 2019). The Swin Transformer has also been explored in the context of UDA, where its ability to model local and global relationships in images is harnessed for domain adaptation. However, most of these methods require additional components or specific training strategies to prevent model collapse in challenging tasks (Liu et al., 2022; Yang et al., 2021a).

3 Method

This section introduces three key modules: the Graph Domain Discriminator (GDD), Adaptive Double Attention (ADA), and Cross-Feature Transform (CFT). GDD models domain relationships using graphs and attention, ADA enhances feature alignment (Deng et al., 2024) via double attention (Zhang et al., 2022), and CFT boosts feature transfer with cross-attention and dynamic gating. Together, they enable efficient domain alignment. The overall architecture is demonstrated in Figure 1.

3.1 Graph Domain Discriminator

The proposed unsupervised domain adaptation method introduces a *Graph Domain Discriminator* (GDD), as shown in Figure 2. The GDD enhances both local and global adaptation by utilizing structural relationships between samples from source and target domains.

For local adaptation, the GDD leverages key features from the third transformer block's attention mechanisms to capture fine-grained details. This includes processing features from windows and

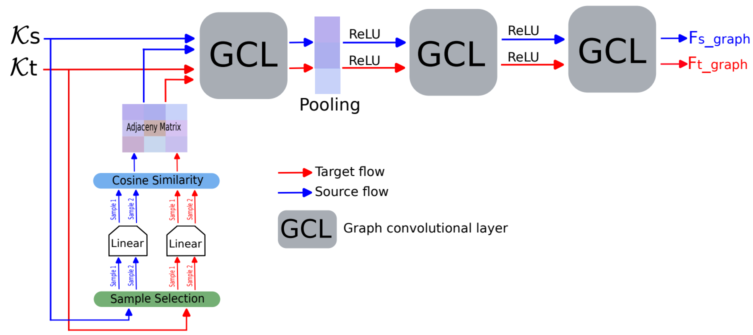

Figure 2: The architecture of the Graph Domain Discriminator uses K_s and K_t to represent source and target key features of MADA, respectively.

shifted windows to align local characteristics, illustrated in Figure 1. For global adaptation, it uses the MLP output from the final transformer block to capture abstract global representations, also depicted in Figure 1. By integrating these strategies, the GDD aligns deep and shallow features, improving the model's generalization across domains.

A vital element of the GDD is the adjacency matrix, which represents the graph structure for convolution operations. It begins with two samples selected by a learnable parameter during training, which are processed through a projection layer $P(\mathbf{x}_{sample_i})$ and $P(\mathbf{x}_{sample_j})$ to fit the adjacency matrix's requirements. The adjacency between samples i and j is defined by cosine similarity:

$$\mathbf{A}_{ij} = \cos(\theta_{ij}) = \frac{P(\mathbf{x}_{sample_i}) \cdot P(\mathbf{x}_{sample_j})}{\|P(\mathbf{x}_{sample_i})\| \|P(\mathbf{x}_{sample_j})\|} \tag{1}$$

Here, $\mathbf{A}_{ij}$ is the adjacency matrix element for samples i and j, and θ_{ij} is the angle between the projected vectors.

The adjacency matrix A is utilized in three layers of graph convolution, each followed by a ReLU activation, facilitating the aggregation of information from individual samples and their neighbors. After the first graph convolutional layer, a pooling operation is applied to reduce the dimensionality and focus on the most salient features, enabling more efficient information processing. To promote domain invariance, a Gradient Reversal Layer (GRL) is introduced, establishing a min-max game between the feature extractor and the domain discriminator. The feature extractor aims to generate features that confuse the discriminator, maximizing the discrepancy for the domain discriminator while minimizing it for the main task, ultimately encouraging the learning of domain-invariant features (Ganin & Lempitsky, 2015).

3.2 Adaptive Double Attention

The adaptive double attention module, shown in Figure 3, processes *windows attention* and *shifted windows attention* simultaneously in each transformer block, termed double attention. It employs a cross-attention mechanism between windows and shifted windows features to enhance alignment and interaction, improving long-range dependency capture and adaptation through dynamic attention re-weighting.

Initially, the module performs feature correction on target domain data to address discrepancies with source features, utilizing a correction block as proposed in (Li et al., 2021a). This block, depicted in Figure 3, modifies the target representation $C^l(F_{x_t, x_{t\_shift}})$ to align it more closely with the source representation, thereby reducing the domain gap and enhancing adaptation.

The correction block consists of two fully connected (FC) layers with ReLU activations. The output of the correction block, $\Delta C^l(F_{x_t, x_{t\_shift}})$, adjusts the representation of the target feature according to the following equation:

$$\hat{C}^l(F_{x_t, x_{t\_shift}}) = C^l(F_{x_t, x_{t\_shift}}) + \Delta C^l(F_{x_t, x_{t\_shift}}) \tag{2}$$

The aim is to make the modified target representation $\hat{C}^l(F_{x_t,x_{t\_shift}})$ similar to the source representation. By doing so, domain alignment is facilitated between $\hat{C}^l(F_{x_t,x_{t\_shift}})$, ensuring that the correction block effectively captures and adjusts discrepancies in the target data to improve the overall adaptation process.

After feature correction, the transformer's attention mechanism processes two feature sets: *windows attention features* and *shifted windows attention features*, represented as Q, K, V and $Q_{shift}, K_{shift}, V_{shift}$, respectively. These matrices correspond to the *query*, *key*, and *value* components of both attention mechanisms (Zhang et al., 2022). By processing them in parallel, the model captures long-range dependencies, enhancing spatial relationship understanding across the image.

Self-attention focuses on windows features, calculating attention via the scaled dot product of Q and K, normalized by feature dimension d. This allows for local dependency enhancement. Cross-attention combines the query from windows attention (Q) with the shifted windows key (K_{shift}) to capture complex spatial relationships. Additionally, both attention types are reweighted using entropy-based scaling to prioritize transferable features and suppress domain-specific ones, further improving long-range dependency processing.

$$\begin{aligned} A &= \frac{QK^T}{\sqrt{d}} \odot H(F_{graph}) \\ A_{shift} &= \frac{QK_{shift}^T}{\sqrt{d}} \odot H(F_{graph}) \end{aligned} \tag{3}$$

Then, the two attention score matrices are concatenated and normalized using the softmax function to produce attention weights (Deng et al., 2024). These final attention weights are applied to the concatenated *value* matrices $[V; V_{shift}]$ to produce the output:

$$\begin{aligned} MADA &= \text{Softmax}(\text{Concat}(A, A_{shift})) \times [V; V_{shift}] \\ Z_{MADA} &= MADA(\text{LN}(Z_{l-1})) + Z_{l-1} \\ Z_l &= \text{MLP}(\text{LN}(Z_{MADA})) + Z_{MADA} \end{aligned} \tag{4}$$

Here, Z_{l-1} represents the input to the Transformer block, Z_{MADA} is output of attention, and Z_l is the output after the multi-head adaptive double attention and feed-forward layers. In the context of the Swin Transformer block, layer normalization (LN) is applied to the input of both the attention and MLP layers. Residual connections are added after each operation, ensuring efficient information flow. This architecture allows the model to effectively learn long-range dependencies through shifted window attention.

By integrating both windows and the shifted windows attention mechanisms and applying entropy-based reweighting, the module captures multiple aspects of the feature representations. This process improves long-range dependencies and allows more effective adaptation across domains, improving overall domain adaptation performance, as supported by (Yang et al., 2023).

The module employs an entropy-based reweighting strategy for both self-attention and cross-attention, reweighting the attention scores using the entropy derived from the *graph domain discriminator* output features. The *entropy function* is defined as:

$$H(F_{graph}) = -\sum_i F_{graph} \log(F_{graph}) \tag{5}$$

The key and shifted key features of the transformer are first processed by the graph domain discriminator, producing outputs $F_{s_{\text{graph}}}$ and $F_{t_{\text{graph}}}$. These outputs are then used to calculate entropy, allowing the module to dynamically reweight attention by emphasizing or suppressing features based on domain-specific importance. This enhances adaptation in unsupervised domain adaptation (Yang et al., 2023) and improves the model's generalization across different domains.

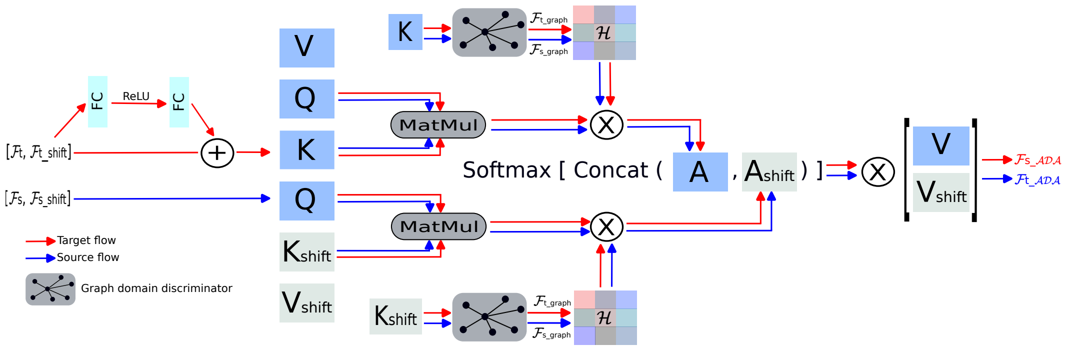

Figure 3: The architecture of Adaptive Double Attention (ADA) module.

3.3 Cross Feature Transform

The proposed Cross Feature Transform (CFT) module enhances domain adaptation within the Transformer architecture by facilitating effective feature alignment between source and target domains. Unlike static methods, the CFT module is applied dynamically after a randomly selected transformer block in each iteration, providing a robust feature transformation approach and reducing the likelihood of overfitting (Sun et al., 2022). The general architecture of the CFT module is illustrated in Figure 4.

Central to the CFT module are bidirectional cross-attention mechanisms, which optimize feature transferability between domains, enabling implicit mixing of features. This enhances the model's ability to learn domain-invariant representations, thereby improving generalization to the target domain (Wang et al., 2022b). The computation of source-to-target attention features F_{s2t} and target-to-source attention features F_{t2s} is performed as follows:

$$\begin{aligned} F_{s2t} &= \text{Softmax}\left(f(X_s)^\top g(X_t)\right) \\ F_{t2s} &= \text{Softmax}\left(g(X_t)^\top f(X_s)\right) \end{aligned} \tag{6}$$

To refine feature alignment, the CFT module incorporates a gating mechanism using a learnable parameter γ, balancing contributions from both directions:

$$\text{Attn}_{gating} = (1 - \sigma(\gamma)) \cdot F_{s2t} + \sigma(\gamma) \cdot F_{t2s} \tag{7}$$

where $\sigma(\gamma)$ is the sigmoid function. This adaptive formulation allows prioritization of source-to-target or target-to-source transformations based on data context.

The pairwise distance between features is computed and combined with the gating attention output:

$$F_{out} = \left(\text{Attn}_{gating} \times \|F_{s2t} - F_{t2s}\|_2^2\right) + X_t \tag{8}$$

Here, $\|F_{s2t} - F_{t2s}\|$ represents the pairwise distance, Attn_{gating} the gating attention output, and X_t is the target feature added as a shortcut.

4 Experiments

4.1 Datasets

We utilize four widely recognized benchmark datasets for our experiments: Office31 (Saenko et al., 2010), Office-Home (Venkateswara et al., 2017), and VisDA-2017 (Peng et al., 2017). Following

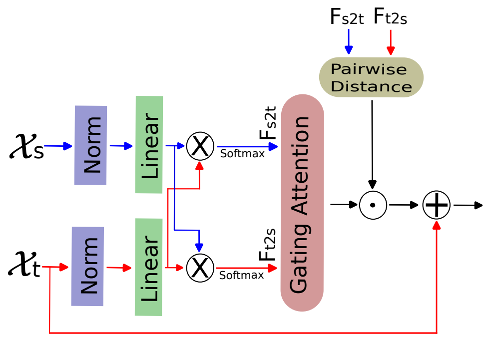

Figure 4: The architecture of Cross Feature Transform (CFT) module. x_s and x_t represents source and target feature, respectively.

the methodology in (Long et al., 2018), we create transfer tasks across these datasets. The Office-31 dataset comprises 4,652 images across 31 categories, divided into three domains: Amazon (A), DSLR (D), and Webcam (W), each sourced from different environments. The Office-Home dataset features images from four domains: Artistic (Ar), Clip Art (Cl), Product (Pr), and Real-World (Rw), each containing 65 categories, thus providing a diverse evaluation benchmark. Lastly, the VisDA-2017 dataset, utilized in the 2018 VisDA challenge, focuses on a synthesis-to-real object recognition task with 12 categories, containing 152,397 synthetic images for the source domain and 55,388 real-world images for the target domain.

4.2 Data Augmentation

We employ CutMix (Yun et al., 2019) and MixUp (Zhang, 2017) as pixel-wise augmentation strategies on raw images to improve feature transferability between domains. Although these methods generally necessitate labeled data, our unsupervised domain adaptation task operates without ground truth labels in the target domain. To tackle this issue, we generate pseudo-labels for the target data using a source-only model trained on the source domain. To reduce noise in these pseudo-labels, we implement a confidence threshold based on the model's accuracy, retaining only predictions that exceed this threshold for the augmentation operations. These augmentations are applied solely to the source data, as our network incorporates a Cross Feature Transform (CFT) module that enhances feature transferability between domains, thus diminishing the necessity for direct augmentation on the target data. The pixel-wise CutMix and MixUp operations, guided by high-confidence pseudo-labels, are illustrated in Figure 1.

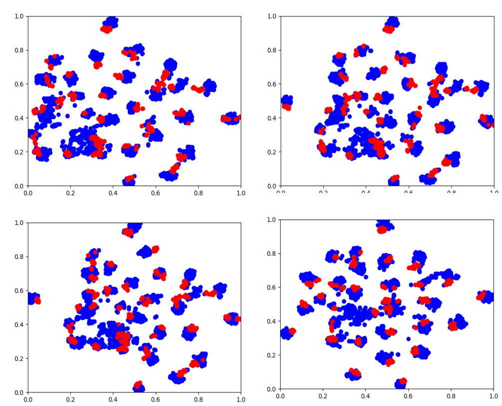

Figure 5: t-SNE visualization of Office-Home dataset, where red and blue points indicate the source and the target domain, respectively. (top left) Swin-B, (top right) +GDD, (bottom left) +CFT, (bottom right) +ADA (TransAdapter)

4.3 Implementation Details

For all domain adaptation (DA) tasks, we utilize the Swin-B model, pretrained on the ImageNet dataset (Deng et al., 2009), as the backbone network in our proposed TransAdapter method, integrating 12 dual transformer blocks from Swin-B within the TransAdapter framework. The model is optimized using the Stochastic Gradient Descent (SGD) algorithm (Bottou, 2010), with a momentum of 0.9 and a weight decay parameter of 1×10^{-3}. We employ a base learning rate of 1×10^{-2} for the Office-31, and Office-Home datasets, while a lower learning rate of 1×10^{-3} is applied for the VisDA-2017 dataset. The learning rate follows a warmup cosine scheduler, gradually increasing during the initial training phase and subsequently decaying throughout the remaining iterations. Across all datasets, the batch size is consistently set to 32, and the model is trained over $15,000$ iterations. The hyperparameters λ_{local}, and λ_{global} in the TransAdapter method are set to 0.1, and 0.01, respectively, for all DA tasks, as shown in Equation 11.

4.4 Objective Function

Our domain adaptive model's objective function combines cross-entropy loss for classification, local adaptation loss (strong alignment), and global adaptation loss (weak alignment) The classification layer is a single fully connected layer. For the labeled source domain, the cross-entropy loss is defined as:

$$L_{\text{cls}} = \text{CE}(G(F_{cls}), y_s) \tag{9}$$

where $G(\cdot)$ normalizes and flattens the transformer features, y_s is the ground truth for the source data, and $\text{CE}(\cdot, \cdot)$ denotes the cross-entropy loss, using only the source domain features F_{cls}.

Local-Global Adaptation Loss: The combined loss function is computed by averaging the cross-entropy loss for local adaptation and the focal loss for global adaptation across both source and target domains:

$$\begin{aligned} L_{local} &= \frac{1}{2}\left(\text{CE}(G(F^{src}_{ADV\_local}), \hat{y}^{src}) + \text{CE}(G(F^{tgt}_{ADV\_local}), \hat{y}^{tgt})\right) \\ L_{global} &= \frac{1}{2}\left(FL(G(F^{src}_{ADV\_global}), \hat{y}^{src}) + FL(G(F^{tgt}_{ADV\_global}), \hat{y}^{tgt})\right) \end{aligned} \tag{10}$$

Where, $\hat{y}^{src}$ and $\hat{y}^{tgt}$ denote the ground truth labels for source and target data, respectively. Specifically, $\hat{y}^{src}$ is set to 1 for source data and $\hat{y}^{tgt}$ is set to 0 for target data. The terms F_{ADV_global} and F_{ADV_local} are illustrated in Figure 1. The function $G(\cdot)$ refers to a flattening operation followed by a fully connected layer. CE represents cross-entropy loss and $FL(\cdot)$ represents focal loss to address class imbalance by down-weighting the contribution of easy-to-classify examples.

The overall objective function is:

$$\mathcal{L}_{\text{total}} = \lambda_{\text{local}}\mathcal{L}_{\text{local}} + \lambda_{\text{global}}\mathcal{L}_{\text{global}} + \mathcal{L}_{\text{classifier}} \tag{11}$$

where λ_{local} and λ_{global} are the coefficients for the respective loss components.

4.5 Results of Object Recognition

Table 2, 3 and 1 present the accuracy results on the Office-31 (Saenko et al., 2010), Office-Home (Venkateswara et al., 2017), and VisDA-2017 (Peng et al., 2017) datasets, respectively. Comparisons are made across multiple backbones, including AlexNet, ResNet, DeiT, Swin, and ViT, with methods such as Source Only, DDC (Tzeng et al., 2014b), DAN (Long et al., 2015a), RevGrad (Ganin & Lempitsky, 2015), FFAN (Chen et al., 2019), TAT (Liu et al., 2019), SHOT (Liang et al., 2020), ALDA (Chen et al., 2020), CDTrans (Xu et al., 2021b), BCAT (Wang et al., 2022b), WinTR (Ma et al., 2021), TVT (Yang et al., 2023), and the proposed TransAdapter.

In Table 2 on the Office-31 (Saenko et al., 2010) dataset, the Swin backbone achieves state-of-the-art performance, particularly excelling in the W $\rightarrow$ D task, where it matches the highest accuracy of 100%. In particular, the proposed TransAdapter model outperforms BCAT (Wang et al., 2022b) in most tasks, leading to an overall average accuracy of 95.5%, compared to BCAT (Wang et al., 2022b) 95.0%.

Table 3 presents the results on the Office-Home (Venkateswara et al., 2017) dataset, where TransAdapter again achieves superior performance with the Swin backbone. It achieves the

Table 1: Accuracy (%) on the VisDA-2017 dataset. "-B" indicates that the backbone is Base, respectively. The best performance is marked as bold.

Method	plane	bcycl	bus	car	house	knife	mcycl	person	plant	sktbrd	train	truck	Avg
ResNet Backbone													
Source Only	55.1	53.3	61.9	59.1	80.6	17.9	79.7	31.2	81.0	26.5	73.5	8.5	52.4
RevGrad Ganin & Lempitsky (2015)	81.9	77.7	82.8	44.3	81.2	29.5	65.1	28.6	51.9	54.6	82.8	7.8	57.4
MCD Saito et al. (2018)	87.0	60.9	83.7	64.0	88.9	79.6	84.7	76.9	88.6	40.3	83.0	25.8	71.9
ALDA Chen et al. (2020)	93.8	74.1	82.4	69.4	90.6	87.2	89.0	67.6	93.4	76.1	87.7	22.2	77.8
DTA Lee et al. (2019)	93.7	82.2	85.6	83.8	93.0	81.0	90.7	82.1	95.1	78.1	86.4	32.1	81.5
SHOT Liang et al. (2020)	94.3	88.5	80.1	57.3	93.1	94.9	80.7	80.3	91.5	89.1	86.3	58.2	82.9
DeiT Backbone													
Source Only-B	97.7	48.1	86.6	61.6	78.1	63.4	94.7	10.3	87.7	47.7	94.4	35.5	67.1
CDTrans-B Xu et al. (2021b)	97.1	90.5	82.4	77.5	96.6	96.1	93.6	88.6	97.9	86.9	90.3	62.8	88.4
Swin Backbone													
Source Only	98.7	63.0	86.7	68.5	94.6	59.4	98.0	22.0	81.9	91.4	96.7	25.7	73.9
BCAT Wang et al. (2022b)	**99.1**	91.6	86.6	72.3	98.7	**97.9**	96.5	82.3	94.2	96.0	**93.9**	61.3	89.2
TransAdapter (ours)	98.6	**94.1**	**88.3**	**75.2**	**98.9**	97.2	**97.9**	**87.1**	**96.8**	**97.7**	93.2	**67.6**	**91.2**
ViT Backbone													
Source Only	98.2	73.0	82.5	62.0	97.3	63.5	96.5	29.8	68.7	86.7	96.7	23.7	73.2
TVT Yang et al. (2023)	97.1	92.9	85.3	66.4	97.1	97.1	89.3	75.5	95.0	94.7	94.5	55.1	86.7

Table 2: Accuracy (%) on the Office-31 dataset. "-S" and "-B" indicates that the backbone is Small and Base, respectively. The best performance is marked as bold.

Method	$A \to W$	$D \to W$	$W \to D$	$A \to D$	$D \to A$	$W \to A$	Avg
AlexNet Backbone							
Source Only	61.6	95.4	99.0	63.8	51.1	49.8	70.1
DDC Tzeng et al. (2014b)	61.8	95.0	98.5	64.4	52.1	52.2	70.6
DAN Long et al. (2015a)	68.5	96.0	99.0	67.0	54.0	53.1	72.9
RevGrad Ganin & Lempitsky (2015)	73.0	96.4	99.2	72.3	53.4	51.2	74.3
FFAN Chen et al. (2019)	83.0	99.0	99.9	76.3	63.3	60.8	80.4
ResNet Backbone							
Source Only	68.4	96.7	99.3	68.9	62.5	60.7	76.1
DDC Tzeng et al. (2014b)	75.6	96.0	98.2	76.5	62.2	61.5	78.3
DAN Long et al. (2015a)	80.5	97.1	99.6	78.6	63.6	62.8	80.4
RevGrad Ganin & Lempitsky (2015)	82.0	96.9	99.1	79.7	68.2	67.4	82.2
TAT Liu et al. (2019)	92.5	99.3	100.0	93.2	73.1	72.1	88.4
SHOT Liang et al. (2020)	90.1	98.4	99.9	94.0	74.7	74.3	88.6
ALDA Chen et al. (2020)	95.6	97.7	100.0	94.0	72.2	72.5	88.7
DeiT Backbone							
Source Only-S	86.9	97.7	99.6	87.6	74.9	73.5	86.7
CDTrans-S Xu et al. (2021b)	93.5	98.2	99.6	94.6	78.4	78.0	90.4
Source Only-B	90.4	98.2	100.0	90.8	76.8	76.4	88.8
CDTrans-B Xu et al. (2021b)	96.7	99.9	100.0	97.0	81.1	81.9	92.6
Swin Backbone							
Source Only	89.2	94.1	100.0	93.1	80.9	81.3	89.8
BCAT Wang et al. (2022b)	**99.2**	**99.5**	100.0	99.6	85.7	86.1	95.0
TransAdapter	99.1	98.9	**100.0**	**99.9**	**88.3**	**87.2**	**95.5**
ViT Backbone							
Source Only	89.2	98.9	100.0	88.8	80.1	79.8	89.5
TVT Yang et al. (2023)	96.4	99.4	100.0	96.4	84.9	86.1	93.9

highest average accuracy of 88.3%, outperforming BCAT (Wang et al., 2022b) and other methods, particularly in the tasks A $\to$ PA and A $\to$ AC, where it records 91.8% and 91.5%, respectively.

Finally, Table 1 highlights the performance on the VisDA-2017 (Peng et al., 2017) dataset. Here, the TransAdapter with the Swin backbone significantly outperforms other methods, achieving the highest average accuracy of 91.2%. It shows remarkable performance in challenging categories such as knife, bcycl, and train, where it meets or exceeds the accuracy of existing state-of-the-art methods.

4.6 Ablation Study

Table 4 presents the results of the ablation study, showcasing the impact of each module on domain adaptation performance. The baseline *Source Only* model achieved an average accuracy of 81.1%.

Table 3: Accuracy (%) on the Office-Home dataset. "-S" and "-B" indicates that the backbone is Small and Base, respectively. The best performance is marked as bold.

Method	$A \rightarrow C$	$A \rightarrow P$	$A \rightarrow R$	$C \rightarrow A$	$C \rightarrow P$	$C \rightarrow R$	$P \rightarrow A$	$P \rightarrow C$	$P \rightarrow R$	$R \rightarrow A$	$R \rightarrow C$	$R \rightarrow P$	Avg
AlexNet Backbone													
Source Only	26.4	32.6	41.3	22.1	41.7	42.1	20.5	20.3	51.1	31.0	27.9	54.9	34.3
DAN Long et al. (2015a)	31.7	43.2	55.1	33.8	48.6	50.8	30.1	35.1	57.7	44.6	39.3	63.7	44.5
RevGrad Ganin & Lempitsky (2015)	36.4	45.2	54.7	35.2	51.8	55.1	31.6	39.7	59.3	45.7	46.4	65.9	47.3
ResNet Backbone													
Source Only	34.9	50.0	58.0	37.4	41.9	46.2	38.5	31.2	60.4	53.9	41.2	59.9	46.1
DAN Long et al. (2015a)	43.6	57.0	67.9	45.8	56.5	60.4	44.0	43.6	67.7	63.1	51.5	74.3	56.3
RevGrad Ganin & Lempitsky (2015)	45.6	59.3	70.1	47.0	58.5	60.9	46.1	43.7	68.5	63.2	51.8	76.8	57.6
SHOT Liang et al. (2020)	57.1	78.1	81.5	68.0	78.2	78.1	67.4	54.9	82.2	73.3	58.8	84.3	71.8
DeiT Backbone													
Source Only-S	55.6	73.0	79.4	70.6	72.9	76.3	67.5	51.0	81.0	74.5	53.2	82.7	69.8
CDTrans-S Xu et al. (2021b)	60.0	79.5	82.4	75.6	81.0	82.3	72.5	56.7	84.4	77.0	59.1	85.5	74.7
Source Only-B	61.8	79.5	84.3	75.4	78.8	81.2	72.8	55.7	84.4	78.3	59.3	86.0	74.8
CDTrans-B Xu et al. (2021b)	68.8	85.0	86.9	81.5	87.1	87.3	79.6	63.3	88.2	82.0	66.0	90.6	80.5
WinTR-S Ma et al. (2021)	65.3	84.1	85.0	76.8	84.5	84.4	73.4	60.0	85.7	77.2	63.1	86.8	77.2
Swin Backbone													
Source Only	64.5	84.8	87.6	82.2	84.6	86.7	78.8	60.3	88.9	82.8	65.3	89.6	79.7
BCAT Wang et al. (2022b)	75.3	90.0	**92.9**	88.6	90.3	**92.7**	87.4	73.7	92.5	86.7	75.4	**93.5**	86.6
TransAdapter	**77.6**	**91.8**	92.8	**91.5**	**92.3**	92.6	**90.3**	**77.6**	92.8	**87.9**	**79.1**	92.8	**88.3**
ViT Backbone													
Source Only	66.2	84.3	86.6	77.9	83.3	84.3	76.0	62.7	88.7	80.1	66.2	88.7	78.7
TVT Yang et al. (2023)	74.9	86.8	89.5	82.8	88.0	88.3	79.8	71.9	90.1	85.5	74.6	90.6	83.6

Adding the Graph Domain Discriminator (GDD) improved accuracy to 84.0%, while incorporating the Cross Feature Transform (CFT) module raised it to 87.4%. The complete model, including the Adaptive Double Attention (ADA) module, achieved the highest accuracy of 91.0%, highlighting the ADA module's role in capturing long-range dependencies. Figure 5 visualizes the domain separation performance of each module using t-SNE on the Office Home dataset, demonstrating improved domain separation with each addition, particularly with the complete model featuring the $+ADA$ module (TransAdapter).

5 Conclusion

In this paper, we introduce TransAdapter, a novel framework that leverages the Swin Transformer for Unsupervised Domain Adaptation (UDA). Our approach features three specialized modules: a graph domain discriminator, adaptive double attention, and cross-feature transform, which enhance the Swin Transformer's ability to capture both shallow and deep features while improving long-range dependency modeling. Experimental results on standard UDA benchmarks show that TransAdapter significantly outperforms existing methods and demonstrates robustness against domain shifts. However, the combined use of window and shifted window attention may increase computational complexity, and our current implementation lacks task-specific adaptation mechanisms for detection and segmentation. Future work will focus on extending the model for these applications and exploring ways to reduce computational complexity while maintaining long-range dependency modeling.

Method	Office-31	Office-Home	VisDA-2017	Avg
Source Only	89.8	79.7	73.9	81.1
+GDA	91.7	81.6	78.8	84.0
+CFT	93.5	84.1	84.6	87.4
+ADA (TransAdapter)	**95.5**	**87.5**	**90.2**	**91.0**

Table 4: Ablation study of each module (%). The best performance is marked as bold. Last row corresponds the proposed model.

References

Léon Bottou. Large-scale machine learning with stochastic gradient descent. In *Proceedings of COMPSTAT'2010*, pp. 177–186. Springer, 2010.

K. Bousmalis et al. Unsupervised domain adaptation by backpropagation. *Journal of Machine Learning Research*, 18:1–35, 2017.

Chaoqi Chen, Weiping Xie, Wenbing Huang, Yu Rong, Xinghao Ding, Yue Huang, Tingyang Xu, and Junzhou Huang. Progressive feature alignment for unsupervised domain adaptation. In *Proceedings of the IEEE/CVF conference on computer vision and pattern recognition*, pp. 627–636, 2019.

Kai Chen, Jiangmiao Wang, Shuo Yang, Yao Guo, Ming Gao, Yu Zou, and Jianxin Yang. Domain adaptive multi-modal transformer for object detection. In *Proceedings of the 29th ACM International Conference on Multimedia (MM)*, pp. 1036–1044, 2021a.

L. Chen et al. Understanding domain adaptation in deep learning. *Artificial Intelligence Review*, 54: 1265–1282, 2021b.

Minghao Chen, Shuai Zhao, Haifeng Liu, and Deng Cai. Adversarial-learned loss for domain adaptation. In *Proceedings of the AAAI conference on artificial intelligence*, volume 34, pp. 3521–3528, 2020.

G. Csurka. Domain adaptation for visual recognition: A comprehensive survey. *arXiv preprint arXiv:1702.05374*, 2017.

Jia Deng, Wei Dong, Richard Socher, Li-Jia Li, Kai Li, and Li Fei-Fei. Imagenet: A large-scale hierarchical image database. *2009 IEEE conference on computer vision and pattern recognition*, pp. 248–255, 2009.

Yingying Deng, Xiangyu He, Fan Tang, and Weiming Dong. Z*: Zero-shot style transfer via attention reweighting. In *Proceedings of the IEEE/CVF Conference on Computer Vision and Pattern Recognition*, pp. 6934–6944, 2024.

J. Devlin et al. Bert: Pre-training of deep bidirectional transformers for language understanding. *arXiv preprint arXiv:1810.04805*, 2018.

A. Dosovitskiy et al. An image is worth 16x16 words: Transformers for image recognition at scale. *arXiv preprint arXiv:2010.11929*, 2020.

Yaroslav Ganin and Victor Lempitsky. Unsupervised domain adaptation by backpropagation. In *International conference on machine learning*, pp. 1180–1189. PMLR, 2015.

Ian Goodfellow, Jean Pouget-Abadie, Mehdi Mirza, Bing Xu, David Warde-Farley, Sherjil Ozair, Aaron Courville, and Yoshua Bengio. Generative adversarial nets. *Advances in Neural Information Processing Systems*, pp. 2672–2680, 2014.

K. Han et al. Generative adversarial transformers. *arXiv preprint arXiv:2008.07772*, 2020.

K. He et al. Masked autoencoders are scalable vision learners. *arXiv preprint arXiv:2111.06377*, 2021.

W. Jiang et al. Improving domain adaptation with pseudo-labels. *Pattern Recognition*, 104:107248, 2020.

W. Jiang et al. Cross-domain learning with deep neural networks. *Pattern Recognition*, 115:107888, 2021.

Yiqi Jiang et al. Domain shift challenges in deep learning. *Neural Computation*, 34:1423–1442, 2022.

G. Kang et al. Deep adaptation networks for domain adaptation. *Journal of Machine Learning Research*, 20:1–30, 2019.

M. Khan et al. Transformers in vision: A survey. *ACM Computing Surveys*, 54:1–41, 2021.

T. Kuroki et al. An overview of unsupervised domain adaptation methods. *Journal of AI Research*, 17:45–67, 2019.

Seungmin Lee, Dongwan Kim, Namil Kim, and Seong-Gyun Jeong. Drop to adapt: Learning discriminative features for unsupervised domain adaptation. In *Proceedings of the IEEE/CVF international conference on computer vision*, pp. 91–100, 2019.

Shuang Li, Binhui Xie, Qiuxia Lin, Chi Harold Liu, Gao Huang, and Guoren Wang. Generalized domain conditioned adaptation network. *IEEE Transactions on Pattern Analysis and Machine Intelligence*, pp. 1–1, 2021a. doi: 10.1109/TPAMI.2021.3062644.

Y. Li et al. Towards robust domain adaptation. *IEEE Transactions on Neural Networks and Learning Systems*, 32:569–583, 2021b.

Jian Liang, Dapeng Hu, and Jiashi Feng. Do we really need to access the source data? source hypothesis transfer for unsupervised domain adaptation. In *International conference on machine learning*, pp. 6028–6039. PMLR, 2020.

Hong Liu, Mingsheng Long, Jianmin Wang, and Michael Jordan. Transferable adversarial training: A general approach to adapting deep classifiers. In *International conference on machine learning*, pp. 4013–4022. PMLR, 2019.

Z. Liu et al. Swin transformer: Hierarchical vision transformer using shifted windows. *arXiv preprint arXiv:2103.14030*, 2021.

Ze Liu, Han Hu, Zheng Zhang, Yutong Lin, Yixuan Wei, and Yue Cao. Swin transformer for domain adaptation. In *Proceedings of the IEEE/CVF Conference on Computer Vision and Pattern Recognition (CVPR)*, pp. 12001–12008, 2022.

Mingsheng Long, Yue Cao, Jianmin Wang, and Michael Jordan. Learning transferable features with deep adaptation networks. In *International conference on machine learning*, pp. 97–105. PMLR, 2015a.

Mingsheng Long, Yue Cao, Jianmin Wang, and Michael I Jordan. Learning transferable features with deep adaptation networks. In *Proceedings of the 32nd International Conference on Machine Learning (ICML)*, pp. 97–105, 2015b.

Mingsheng Long, Han Zhu, Jianmin Wang, and Michael I Jordan. Deep transfer learning with joint adaptation networks. In *Proceedings of the 34th International Conference on Machine Learning (ICML)*, pp. 2208–2217, 2017.

Mingsheng Long, Zhangjie Cao, Jianmin Wang, and Michael I Jordan. Conditional adversarial domain adaptation. *Advances in neural information processing systems*, 31, 2018.

Wenxuan Ma, Jinming Zhang, Shuang Li, Chi Harold Liu, Yulin Wang, and Wei Li. Exploiting both domain-specific and invariant knowledge via a win-win transformer for unsupervised domain adaptation. *arXiv preprint arXiv:2111.12941*, 2021.

P. Morerio et al. Noisy labels in domain adaptation: A robust approach. *IEEE Transactions on Pattern Analysis and Machine Intelligence*, 42:2051–2064, 2020.

P. Oza et al. Efficient domain adaptation with deep learning. *IEEE Transactions on Cybernetics*, 51: 812–825, 2021.

Xingchao Peng, Ben Usman, Neela Kaushik, Judy Hoffman, Dequan Wang, and Kate Saenko. Visda: The visual domain adaptation challenge. In *arXiv preprint arXiv:1710.06924*, 2017.

Y. Qian et al. Recent advancements in deep neural networks for computer vision. *IEEE Transactions on Pattern Analysis and Machine Intelligence*, 43(8):2456–2473, 2021.

Kate Saenko, Brian Kulis, Mario Fritz, and Trevor Darrell. Adapting visual category models to new domains. In *European Conference on Computer Vision*, pp. 213–226. Springer, 2010.

Kuniaki Saito, Kohei Watanabe, Yoshitaka Ushiku, and Tatsuya Harada. Maximum classifier discrepancy for unsupervised domain adaptation. In *Proceedings of the IEEE conference on computer vision and pattern recognition*, pp. 3723–3732, 2018.

Kuniaki Saito, Yoshitaka Ushiku, Tatsuya Harada, and Kate Saenko. Domain adaptation with multi-branch generative networks. In *Proceedings of the IEEE/CVF Conference on Computer Vision and Pattern Recognition (CVPR)*, pp. 3699–3708, 2019.

Tao Sun, Cheng Lu, Tianshuo Zhang, and Haibin Ling. Safe self-refinement for transformer-based domain adaptation. In *Proceedings of the IEEE/CVF conference on computer vision and pattern recognition*, pp. 7191–7200, 2022.

M. Tan et al. A survey on deep learning for computer vision applications. *Neurocomputing*, 354: 30–44, 2019.

Eric Tzeng, Judy Hoffman, Kate Saenko, and Trevor Darrell. Deep domain confusion: Maximizing for domain invariance. In *arXiv preprint arXiv:1412.3474*, 2014a.

Eric Tzeng, Judy Hoffman, Ning Zhang, Kate Saenko, and Trevor Darrell. Deep domain confusion: Maximizing for domain invariance. *arXiv preprint arXiv:1412.3474*, 2014b.

Eric Tzeng, Judy Hoffman, Kate Saenko, and Trevor Darrell. Adversarial discriminative domain adaptation. In *Proceedings of the IEEE Conference on Computer Vision and Pattern Recognition (CVPR)*, pp. 7167–7176, 2017.

A. Vaswani et al. Attention is all you need. *Advances in Neural Information Processing Systems*, 30:5998–6008, 2017.

Hemanth Venkateswara, Jose Eusebio, Shayok Chakraborty, and Sethuraman Panchanathan. Deep hashing network for unsupervised domain adaptation. In *Proceedings of the IEEE Conference on Computer Vision and Pattern Recognition*, pp. 5018–5027, 2017.

R. VS et al. A comprehensive survey on unsupervised domain adaptation. *IEEE Transactions on Neural Networks and Learning Systems*, 32:800–818, 2021.

X. Wang et al. Deep neural networks in machine learning tasks. *Journal of Machine Learning Research*, 23:1–15, 2022a.

Xiyu Wang, Pengxin Guo, and Yu Zhang. Domain adaptation via bidirectional cross-attention transformer. *arXiv preprint arXiv:2201.05887*, 2022b.

G. Wilson and D. Cook. Domain adaptation in deep learning: A survey. *IEEE Transactions on Neural Networks and Learning Systems*, 31:2031–2043, 2020.

Rui Xu, Lianzhi Ke, Shaogang Zhang, and Xin Zhao. Cdtrans: Cross-domain transformer for unsupervised domain adaptation. In *arXiv preprint arXiv:2109.06165*, 2021a.

Tongkun Xu, Weihua Chen, Pichao Wang, Fan Wang, Hao Li, and Rong Jin. Cdtrans: Cross-domain transformer for unsupervised domain adaptation. *arXiv preprint arXiv:2109.06165*, 2021b.

Jinyu Yang, Jingjing Liu, Ning Xu, and Junzhou Huang. Tvt: Transferable vision transformer for unsupervised domain adaptation. In *Proceedings of the IEEE/CVF Winter Conference on Applications of Computer Vision*, pp. 520–530, 2023.

Liu Yang, Yule Song, Shaogang Zhang, Xin Zhao, and Hao Su. Multi-level domain adaptation using vision transformer. In *arXiv preprint arXiv:2110.03058*, 2021a.

Shuang Yang, Linchao Liu, Dezhong Chen, Minghai Tang, Wengang Zhang, and Wanli Ouyang. Transferable vision transformers with token partitioning and domain re-weighting. In *arXiv preprint arXiv:2109.02796*, 2021b.

Sangdoo Yun, Dongyoon Han, Seong Joon Oh, Sanghyuk Chun, Junsuk Choe, and Youngjoon Yoo. Cutmix: Regularization strategy to train strong classifiers with localizable features. In *Proceedings of the IEEE/CVF international conference on computer vision*, pp. 6023–6032, 2019.

Bowen Zhang, Shuyang Gu, Bo Zhang, Jianmin Bao, Dong Chen, Fang Wen, Yong Wang, and Baining Guo. Styleswin: Transformer-based gan for high-resolution image generation. In *Proceedings of the IEEE/CVF conference on computer vision and pattern recognition*, pp. 11304–11314, 2022.

Hongyi Zhang. mixup: Beyond empirical risk minimization. *arXiv preprint arXiv:1710.09412*, 2017.

W. Zhang et al. Category-level domain adaptation for neural networks. *IEEE Transactions on Neural Networks and Learning Systems*, 30:277–287, 2019.

W. Zhang et al. Learning transferable features with deep adaptation networks. *IEEE Transactions on Neural Networks and Learning Systems*, 31:812–825, 2020.

H. Zhao et al. Domain adaptation challenges in deep neural networks. *IEEE Transactions on Neural Networks and Learning Systems*, 31:2031–2043, 2020.